

Absence of low temperature anomaly in the Debye-Waller factor of solid ^4He

E. Blackburn,¹ J. M. Goodkind,¹ S. K. Sinha,¹ J. Hudis,² C. Broholm,²
J. van Duijn,³ C. D. Frost,⁴ O. Kirichek,⁴ and R. B. E. Down⁴

¹*Physics Department, University of California, San Diego, 9500 Gilman Drive, La Jolla, California 92093*

²*Department of Physics and Astronomy, The Johns Hopkins University, Baltimore, Maryland 21218*

³*Departamento de Química Inorgánica I, Facultad de Ciencias Químicas,
Universidad Complutense de Madrid, 28040 Madrid, Spain*

⁴*ISIS Facility, Rutherford-Appleton Laboratory, Chilton, Didcot, OX11 0QX, United Kingdom*

(Dated: May 26, 2019)

The mean square atomic displacement in hcp-phase solid ^4He has been measured in crystals with a molar volume of 21.3 cm^3 . It is temperature independent from 1 K to 140 mK, with no evidence for an anomaly in the vicinity of the proposed supersolid transition. The mean square displacement is different for in-plane motions ($0.122 \pm 0.001 \text{ \AA}^{-2}$) and out-of-plane motions ($0.150 \pm 0.001 \text{ \AA}^{-2}$).

PACS numbers: 67.80.-s, 67.80.Cx, 61.12.Ld

The recent experiments by Kim and Chan [1, 2] on hexagonal close packed (hcp) solid ^4He have re-opened interest in the old question of supersolidity. In the 1970s, several theorists considered whether the formation of a Bose-Einstein condensate was possible in the presence of a crystalline lattice [3, 4, 5] and Leggett [5] predicted a signature in the rotational inertia. Kim and Chan observed just such a shift, and this has subsequently been reproduced by several groups (e.g. Ref. 6). The transition temperature observed by Kim and Chan ($\sim 200 \text{ mK}$) is close to an anomaly previously observed by Ho *et al.* [7] in the acoustic attenuation in solid ^4He crystals. Ho *et al.* ascribed this anomaly to a change in the behaviour of defects in the crystal, and it is thought that defects may play an important role in supersolid formation [3].

To investigate this in more detail, we have carried out neutron diffraction experiments on solid ^4He crystals to look for traces of a supersolid transition. The neutron diffraction cross section is proportional to the squared Fourier transform of the nuclear density distribution in space and time. If the nuclei form a crystal lattice, then this Fourier transform yields Bragg peaks with an intensity that is proportional to the unit cell structure factor and the Debye-Waller factor from which the mean square displacement of the ^4He nuclei can be extracted. We note that even non-solid samples may have a periodic density distribution and hence Bragg peaks. To narrow the options for the origin of the recently detected anomalies in hcp helium it is important to determine the degree to which the nuclear density distribution is affected in this temperature range. In particular it is of interest to probe the mean squared nuclear displacement, accessible through the Debye-Waller factor.

He crystals were prepared in a cylindrical stainless steel sample chamber (height 32.1 mm, diameter 33.5 mm) equipped with quartz transducers to monitor ultrasound propagation through the growing crystal. ^4He gas, contaminated with a trace amount of ^3He [6, 7], was supplied and pressurized through a stainless steel capillary located

at the top of the sample chamber. The sample chamber was cooled using an Oxford Instruments dilution refrigerator, wherein thermal contact to the mixing chamber was established using a Cu wire attached to the bottom of the sample chamber. The sample chamber supported growth of multiple crystallites with different orientation as opposed to a single crystalline sample.

The dilution refrigerator used for the measurements had difficulty cooling to 1 K when the filling capillary to the sample chamber was filled with liquid. Therefore, the solid had to be formed at higher temperature and pressure. The sample examined here was formed by starting at pressure $p = 45 \text{ bar}$ and temperature $T \sim 2 \text{ K}$. Solid ^4He was then grown using the ‘blocked capillary technique’, in which a solid plug is formed in the capillary as the system is cooled so that the molar volume of the sample remains constant as it cools along the melting curve. This means that our sample passed through the region of bcc phase on the melting curve [8], which presumably contributed to the formation of a multi-crystalline sample.

The neutron data were collected using the MAPS instrument at the ISIS Facility, Rutherford Appleton Laboratory, Oxford. MAPS is a time-of-flight spectrometer equipped with approximately 16 m^2 of position sensitive detectors located 6 m from the sample. The instrument was operated in time-of-flight Laue mode with a white pulsed incident beam and the sample fixed in place. Diffraction patterns were obtained over the temperature range 140 mK - 800 mK. At the end of the experiment the sample can was evacuated and an empty can measurement was acquired at 1 K. A standard vanadium sample was also measured to obtain information on the wavelength dependent detector efficiency.

To assess the mean square displacement, multiple peaks from the same crystallite are required, preferably over a large range of momentum transfer. Due to the presence of multiple crystallites in the sample can, it was impractical to identify peaks from the same crystallite

at different locations on the detector. However, because we used a pulsed white incident beam, higher-order reflections from the same crystallite appeared in the same detector pixels, separated by the recorded time-of-flight. For these higher-order reflections to be visible, the principal reflection must be sufficiently strong. 45 reflections were indexed on the basis of their d -spacings, assuming an hcp structure. Peaks of the types (002), (100), (101) and (102) were readily identified, but only peaks of the type (002) and (100) were strong enough for the corresponding higher-order reflections (004) and (200) to be visible at half the time-of-flight.

The molar volume was determined from a range of the plane spacings obtained here, even though the peaks were not from the same crystallites. We found $a = 3.68(1)$ Å and $c = 6.03(1)$ Å, corresponding to a molar volume of $21.3(1)$ cm³. The c/a ratio is 1.638(5) as compared with the ideal hcp ratio of 1.633. This is consistent with expectations from the temperature and pressure during the crystal growth process [9].

Once these peaks were identified, the time-of-flight spectra in the corresponding pixels were normalized to monitor and the empty can measurement subtracted. At small momentum transfers, where the majority of scattering from the can and cryostat was found, a small amount of background scattering remained after this subtraction. An additional subtraction was made when integrating over reflections by taking a slice from the same pixel over a d -spacing range close to that of interest. At higher momentum transfers, the initial subtraction is adequate.

The integrated intensities were then corrected for (i) angular effects, (ii) detector efficiency and (iii) the wavelength dependence of the incident beam flux. To establish the first correction factor, consider a diffraction peak with a scattering angle $2\theta_B$ acquired on a 2D plate a distance Z from the sample. The centre of the detector plate coincides with the centre of an orthonormal coordinate system where $\hat{\mathbf{x}}$ and $\hat{\mathbf{y}}$ are perpendicular directions in the plane of the detector, and $\hat{\mathbf{z}}$ is perpendicular to the plate. The reflection is observed at point (\mathbf{x}, \mathbf{y}) on the plate, and distance from the centre of the sample to this point is $R = (\mathbf{x}^2 + \mathbf{y}^2 + Z^2)^{1/2}$.

The number of neutrons counted in the Bragg peak is

$$I = \frac{d\sigma}{d\Omega} \cdot \Delta\Omega \cdot \Phi \quad (1)$$

where Φ is the incident flux on the sample (neutrons / unit area / unit time), and $\Delta\Omega$ is the solid angle subtended by the sample. We convert this to an integral form; the solid angle can be written as $(d\mathbf{S} \cdot \mathbf{R})/R^3 = d\mathbf{x}d\mathbf{y}Z/R^3$. The incident flux can be written as a function of the incident wavelength - any variation from unity here is accounted for when the vanadium scans are con-

sidered.

$$\Phi = I(\lambda)d\lambda = \frac{\lambda^2 I(\lambda)}{2\pi} dk \quad (2)$$

The neutron scattering cross-section is given by

$$\frac{d\sigma}{d\Omega} = (2\pi)^3 N |F(\boldsymbol{\tau})|^2 \delta(\mathbf{Q} - \boldsymbol{\tau}) \quad (3)$$

where N is the number of unit cells divided by the volume of a unit cell, and is particular to each crystallite, and $|F(\boldsymbol{\tau})|^2$ is the structure factor of the Bragg peak. We therefore arrive at the following expression for the intensity of the Bragg peak at reciprocal lattice vector $\boldsymbol{\tau}$.

$$I_B = (2\pi)^3 N |F(\boldsymbol{\tau})|^2 \frac{\lambda^2 I(\lambda)}{2\pi} \frac{Z}{R^3} \int \int \int \delta(\mathbf{Q} - \boldsymbol{\tau}) d\mathbf{x}d\mathbf{y}dk \quad (4)$$

This integral can be evaluated in momentum space, giving

$$I_B = 2N |F(\boldsymbol{\tau})|^2 d_{hkl}^2 \lambda^2 I(\lambda). \quad (5)$$

This expression applies identically to all of the detector banks. The value of d_{hkl} for the main peaks was obtained by fitting the peak profile as a Gaussian and taking the central value. This value was then halved for the relevant higher-order peak.

To correct for the other factors, the vanadium scan was used. Vanadium is a uniform scatterer, and so Eq. (1) gives

$$\begin{aligned} I_{\text{vana}} &= \frac{\sigma_v}{4\pi} I(\lambda) \Delta\lambda \Delta A_d \frac{Z}{R^3} \\ &= \frac{\sigma_v}{4\pi} \frac{\Delta A_d}{Z^2} \cos^3 2\theta_B \sin \theta_B I(\lambda) \Delta d \end{aligned} \quad (6)$$

where $\sigma_v = 5.08 \cdot 10^{-28}$ m² [10] is the incoherent cross-section for vanadium, $Z = 6.0031$ m, and $\Delta A_d = N_p \Delta x \Delta y$ is the relevant area of the detector. This may be comprised of N_p pixels. For one pixel $\Delta x = 0.025$ m (detector tube diameter) and $\Delta y = 0.015$ m (vertically resolvable distance). Eq. 6 allows $I(\lambda)$ to be extracted from the white beam vanadium diffraction data.

In the harmonic approximation, the structure factor $|F(\boldsymbol{\tau})|^2$ is related to the mean-square displacement as follows

$$F(\boldsymbol{\tau}) = b_{He} \sum_i \exp(i\boldsymbol{\tau} \cdot \mathbf{d}_i) \exp(-W_{\mathbf{d}_i}(\boldsymbol{\tau})). \quad (7)$$

Here \mathbf{d}_i is the position of the i^{th} atom in the unit cell, $b_{He} = 3.26 \cdot 10^{-15}$ m is the scattering length of He⁴ [10], $W_{\mathbf{d}_i}(\boldsymbol{\tau}) = \langle (\boldsymbol{\tau} \cdot \mathbf{u})^2 \rangle$, and \mathbf{u} is the displacement from the average periodic lattice for a specific nucleus [11]. For the He hcp crystal, following Squires [11], the lowest order expansion of the mean square displacement can be broken down into in-plane and out-of-plane (\parallel to c) components, as follows

$$\langle (\boldsymbol{\tau} \cdot \mathbf{u})^2 \rangle = \tau^2 [\langle u_{\parallel}^2 \rangle (\hat{\boldsymbol{\tau}} \cdot \hat{e})^2 + \langle u_{\perp}^2 \rangle (1 - (\hat{\boldsymbol{\tau}} \cdot \hat{e})^2)]. \quad (8)$$

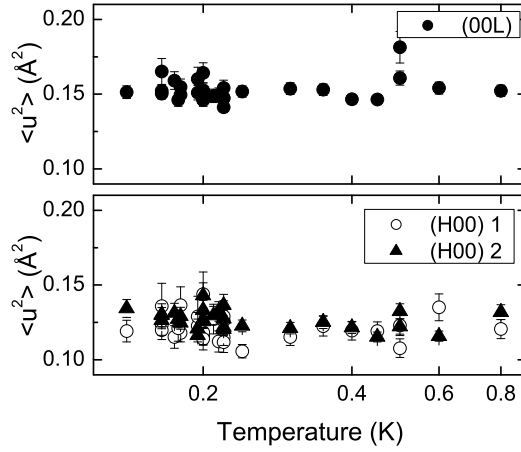


Figure 1: The mean square displacement, $\langle u^2 \rangle$, of ^4He hcp crystal, as measured for the three selected peaks as a function of temperature.

Previous studies have found this expression to be quite adequate for describing the observed data [12, 13].

Hcp He has two atoms per unit cell, and due to symmetry equivalence $W_{\mathbf{d}_i}$ has no site dependence, so

$$|F(\tau)|^2 = b_{He}^2 |\exp(-W_{\mathbf{d}_i})|^2 \left(\sum_i \exp(i\tau \cdot \mathbf{d}_i) \right)^2 \quad (9)$$

After making these corrections, one obtains

$$|\exp(-W_{\mathbf{d}_i})|^2 = \frac{I_{\text{corr}}}{N} \quad (10)$$

where $I_{\text{corr}} = C(I_B/I_{\text{vana}})$ is the corrected intensity of each peak, and C is a correction factor obtained from Eqs. 5, 6 and 9.

We therefore have

$$\ln I_{\text{corr}} = \ln N - 2Q^2 [\langle u_{\parallel}^2 \rangle (\hat{\mathbf{Q}} \cdot \hat{\mathbf{c}})^2 + \langle u_{\perp}^2 \rangle (1 - (\hat{\mathbf{Q}} \cdot \hat{\mathbf{c}})^2)] \quad (11)$$

and so the mean square displacement can be determined from a simple linear fit.

The level of thermal diffuse scattering contributing to the extracted Bragg intensities was calculated following the algorithm developed by Popa and Willis [14] for time-of-flight neutron diffractometry, using phonon velocities measured by Minkiewicz *et al.* [15], and found to be negligible.

Three peaks met the conditions established above, and values for $\langle u^2 \rangle$ were obtained at each temperature considered. Figures 1 and 2 show the temperature dependence of $\langle u^2 \rangle$ and $\ln N$. No thermal anomaly indicative of a phase transition is observed. Table I averages over all of the temperatures assuming no temperature dependence. $\langle u^2 \rangle$ is higher for the (00L) peaks than for the (H00) peaks indicating some anisotropy. The similar values of

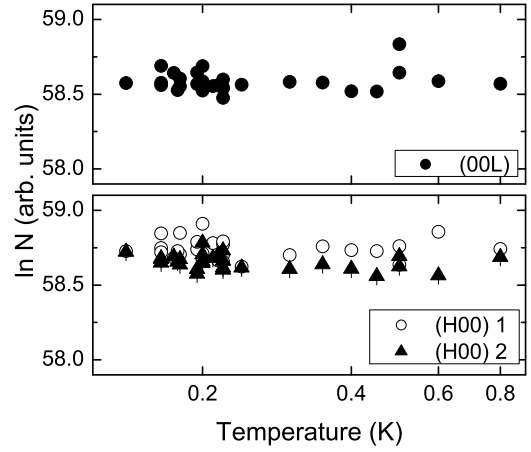


Figure 2: The crystallite dependent quantity $\ln N$, as measured from ^4He hcp crystal for the three selected peaks as a function of temperature.

$\ln N$ indicate similar crystallite sizes. Consideration of the actual peak positions on the detector indicate that the second and third peaks are (100) type peaks could be from the same crystallite, while the (002) type peak is from a different crystallite.

Figure 3 shows the temperature dependence of the lattice parameter a [c] as measured from the (100) [(002)] reflection. Although the lattice parameters for a given crystallite remained fairly stable as a function of temperature, due to different annealing conditions and difficulties with temperature stability between different runs, there was some change in the values obtained. This is most clearly obvious in the upper panel of Figure 3, where two regimes are visible. The upper set of points, which differ from the rest by 1 part in 6000, correspond to conditions where the stress on the crystal was believed to be slightly different to that present for the other measured points. These changes had little impact on the observed mean square displacement, indicating that we are observing the (temperature- and volume-independent) zero-point motion here.

Table II lists published data for $\langle u^2 \rangle$ at different molar volumes. The form for the Debye-Waller factor is different for each reference, and so the values have been converted to the definition of $\langle u^2 \rangle$ given above. These values compare well with theoretically calculated numbers; the value for a crystal of molar volume 15.72 cm^3 is reproduced very well by path-integral Monte Carlo techniques [18], and the value at 20.9 cm^3 is close to that found by Whitlock *et al.* using the Green's function Monte Carlo method [19]. Some estimates were obtained from inelastic neutron scattering studies of the phonons, but the validity of these estimates have been called into doubt by Burns and Isaacs [17], who claim that the phonon data suffer from significant multiple scattering and are

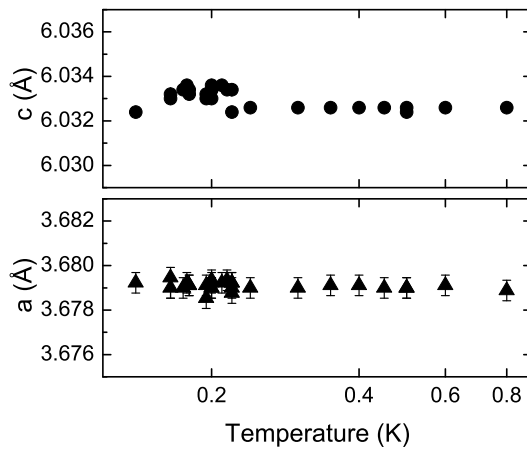


Figure 3: The temperature dependence of the c and a lattice parameters from two of the crystallites studied in the text.

	Peak	d -spacing (Å)	$2\theta_B$ (°)	$\langle u^2 \rangle$ (Å 2)	$\ln N$
1	002	3.016	20.6	0.150 ± 0.001	58.560 ± 0.002
2	100	3.188	18.8	0.118 ± 0.001	58.716 ± 0.003
3	100	3.186	19.7	0.125 ± 0.001	58.636 ± 0.002

Table I: Characteristic properties of the peaks examined on MAPS.

not included.

We have observed a certain amount of anisotropy between in-plane and out-of-plane displacements. The in-plane value is 20 % smaller than the out-of-plane value, indicating that atomic motion is easier out-of-plane. This is not unexpected for an hcp structure, particularly as the close packing is not perfect, and the qualitative behaviour agrees with that calculated by Reese *et al.* [20] from phonon frequencies. The previous x-ray study by Venkataraman and Simmons [12] did not report any anisotropy in the hcp phase, but the reflections studied are not noted. Venkataraman and Simmons noted a decrease in $\langle u^2 \rangle$ as the temperature dropped in the fcc solid phase. We see no temperature dependence, which implies that we are looking at quantum fluctuations.

The principal result is that the mean square displacement does not change in the region of the proposed supersolid transition. In fact, there is no apparent temperature dependence at all over the temperature range studied. The transition, if it exists, does not affect the crystalline lattice significantly. We have also observed a measure of anisotropy between in-plane and out-of-plane motions.

We would like to thank the staff at the ISIS Facility, Rutherford Appleton Laboratory, Oxford, for their assis-

Molar volume (cm 3)	Temp. (K)	$\langle u^2 \rangle$ (Å 2)	Peak type	Reference
11.01	15	0.0593(1)	mixed	Ref. 12 (x-ray)
12.06	5.8	0.0466(3)	mixed	Ref. 13 (neutron)
12.12	14.8	0.0563(14)	mixed	Ref. 16 (x-ray)
12.13	14.8	0.0513(10)	mixed	Ref. 16 (x-ray)
15.72	5.8	0.0861(9)	mixed	Ref. 13 (neutron)
20.9	1.5	0.1537(7)	(00L)	Ref. 17 (x-ray)
21.3	<1	0.150(1)	(00L)	this work (neutron)
21.3	<1	0.122(1)	(H00)	this work (neutron)

Table II: Published values for $\langle u^2 \rangle$ in solid ^4He obtained by x-ray and neutron diffraction. In all cases, the harmonic approximation is assumed and for the mixed peak data, no distinction between in-plane and out-of-plane displacements were made.

tance with the low-temperature and pressure equipment needed.

- [1] E. Kim and M. H. W. Chan, *Nature* **427**, 225 (2004).
- [2] E. Kim and M. H. W. Chan, *Science* **305**, 1941 (2004).
- [3] A. Andreev and I. M. Lifshitz, *Sov. Phys. JETP* **29**, 1007 (1969).
- [4] G. V. Chester, *Phys. Rev. A* **2**, 256 (1970).
- [5] A. J. Leggett, *Phys. Rev. Lett.* **25**, 1543 (1970).
- [6] A. S. C. Rittner and J. D. Reppy, *Phys. Rev. Lett.* **97**, 165301 (2006).
- [7] P.-C. Ho, I. P. Bindloss and J. M. Goodkind, *J. Low Temp. Phys.* **109**, 409 (1997).
- [8] J. H. Vignos and H. A. Fairbank, *Phys. Rev. Lett.* **6**, 265 (1961).
- [9] C. A. Swenson, *Phys. Rev.* **79**, 626 (1950).
- [10] Neutron Data Booklet, Eds. A.-J. Dianoux and G. H. Lander, Old City Publishing (2003).
- [11] G. L. Squires *Introduction to the Theory of Thermal Neutron Scattering* Section 3.6, Cambridge University Press (1978).
- [12] C. T. Venkataraman and R. O. Simmons, *Phys. Rev. B* **68**, 224303 (2003).
- [13] C. Stassis, D. Khatamian and G. R. Kline, *Solid State Comms.* **25**, 531 (1978).
- [14] N. C. Popa and B. T. M. Willis, *Acta Cryst. A* **53**, 537 (1997).
- [15] V. J. Minkiewicz, T. A. Kitchens, F. P. Lipschultz, R. Nathans and G. Shirane, *Phys. Rev.* **174**, 267 (1968).
- [16] D. A. Arms, Ph. D Thesis, University of Illinois at Urbana-Champaign (1999).
- [17] C. A. Burns and E. D. Isaacs, *Phys. Rev. B* **55**, 5767 (1997).
- [18] E. W. Draeger and D. M. Ceperley, *Phys. Rev. B* **61**, 12094 (2000).
- [19] P. A. Whitlock, D. M. Ceperley, G. V. Chester and M. H. Kalos, *Phys. Rev. B* **19**, 5598 (1979).
- [20] R. A. Reese, S. K. Sinha, T. O. Brun and C. R. Tilford, *Phys. Rev. A* **3**, 1688 (1971).